An approach to investigate the multiple-scattering problems based on the singularity expansion method

Pei Cao, Jiu Hui Wu, Xu Chen, and Zhen Huang

Citation: Journal of Applied Physics **123**, 135107 (2018); doi: 10.1063/1.5018478
View online: https://doi.org/10.1063/1.5018478
View Table of Contents: http://aip.scitation.org/toc/jap/123/13
Published by the American Institute of Physics

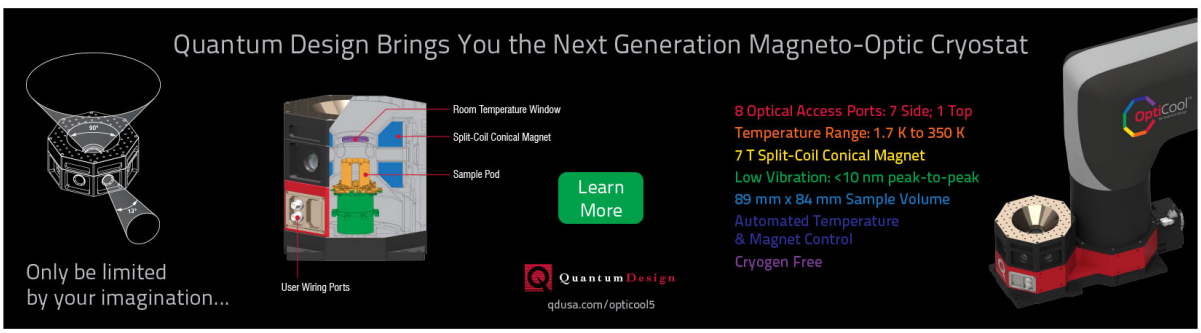

An approach to investigate the multiple-scattering problems based on the singularity expansion method

Pei Cao,[a] Jiu Hui Wu,[b] Xu Chen, and Zhen Huang
School of Mechanical Engineering and State Key Laboratory for Strength and Vibration of Mechanical Structures, Xi'an Jiaotong University, Xi'an 710049, China

(Received 7 December 2017; accepted 23 March 2018; published online 6 April 2018)

An approach to perform the multiple-scattering calculations of the two-cylinder acoustic scattering problem is studied here. The coupling factors and the analytical solutions of the poles are extracted by using the singularity expansion method (SEM). Through interpreting the coupling characteristic of the external oscillations, the poles are also obtained which are consistent with the exact results. It is noted that the coupling characteristic of the scattering field is the corresponding coupling between the oscillation modes of the same order, as well as the SEM poles. Based on this, we then infer that by interpreting the physical meaning of the coupling coefficients and explaining the influence of the coupling characteristic on the SEM poles, the pole distributions and the external oscillation characteristics of multiple scatterers can be studied in acoustic scattering problems. The study is based on general models, and then takes a two-same-cylinder model as an example for comparative analysis. In addition, the relationship between the real parts of the SEM poles and the separated distance is also analyzed briefly. The new approach and the related calculation results provide an effective way to perform shape recognition in the acoustic scattering field. *Published by AIP Publishing.*
https://doi.org/10.1063/1.5018478

I. INTRODUCTION

Multiple scattering problems by two-cylinder systems have been investigated in many fields of physics, for instance, in quantum mechanics, electromagnetism, optics, and acoustics. Many semiclassical methods have been carried out in the past to study such problems.[1] A completely general matrix formulation of the multiple-scattering equations was given by Burke *et al.*[2,3] After that, Young and Bertrand performed the multiple-scattering calculations of the backscattering by two parallel, rigid cylinders, using both direct matrix inversion and an iterative procedure.[4] Another very powerful method is the geometrical theory of diffraction (GTD), which describes the evolution of waves in terms of rays.[1,5] After this theory was put forward, it has been used to take account of the diffraction effects due to creeping waves. Furthermore, Wirzba gave approximations in terms of periodic orbits for any geometry of a finite number of nonoverlapping disks,[6–8] and Gabrielli and Mercier provided an approach to extract and interpret all the scattering resonances of the two impenetrable cylinder scattering problem.[1]

Obviously, the couplings of multiple scatterers cannot be ignored, especially when they are relatively close to each other. The couplings produced by external oscillations have huge impacts on both scattering characteristics and pole distributions of scatterers.[9] In our previous studies, we have already obtained the pole distributions in the acoustic scattering problem by using the singularity expansion method (SEM) and established the relationship between the positions of SEM poles and the geometrical characteristics of single scatterers.[10] However, the couplings of external oscillations will be reflected in the change in the SEM-pole distributions and produce new problems in target recognition. In order to identify the shape characteristics of each scatterer and the distance between multiple scatterers, we need to understand the coupling characteristics of external oscillations using multiple scatterer systems, which mean the variations and distributions of the oscillation frequencies in the presence of couplings.

In this paper, we propose an approach to perform the multiple-scattering calculations of a two-cylinder acoustic scattering problem, extract the coupling factors, and interpret the coupling characteristics of the external oscillations. What is more, the pole distributions of the two-cylinder acoustic scattering problem can be obtained by using the singularity expansion method, and the influence of coupling characteristics on the pole distributions can be then explained. Thus, we can identify the distance between the two scatterers and lay the foundation for further shape recognition of multiple acoustic scatterers.

II. FIRST STEP: COUPLING CHARACTERISTIC EXTRACTION

To obtain the positions of the SEM poles and analyze the influence of couplings, the coupling characteristics are extracted primarily. This section is organized as follows: firstly, the theoretical analysis is briefly reviewed to make clear the specific form of the multiple-scattering equations we have used, and then the coupling coefficients can be derived with an interpretation of their physical meaning through the singularity expansion method.

A. The scattering characteristics of the two-cylinder system

Consider two infinite and parallel cylinders with a center-to-center distance L. The radii of the two cylinders are a

[a]E-mail: yubuyao@yeah.net
[a]Author to whom correspondence should be addressed: ejhwu@mail.xjtu.edu.cn

and b, respectively; the incident wave makes an angle φ' with the X-axis, and the boundary conditions can be divided into two kinds: two rigid cylinders and two ideally soft cylinders. The geometrical situation is shown in Fig. 1. The incident acoustic field can be expressed in the two coordinate systems as follows:[10–13]

$$P_A^i(\rho,\varphi) = \mathrm{e}^{-jk\rho\cos(\varphi-\varphi')} = \sum_{n=-\infty}^{+\infty} j^{-n}\mathrm{J}_n(k\rho)\mathrm{e}^{jn(\varphi-\varphi')}, \quad (1a)$$

$$P_B^i(\rho',\theta) = \mathrm{e}^{-jk\rho'\cos(\theta-\varphi')} = \sum_{n=-\infty}^{+\infty} j^{-n}\mathrm{J}_n(k\rho')\mathrm{e}^{jn(\theta-\varphi')}, \quad (1b)$$

where the wavenumber $k = \omega/c$, $\mathrm{J_n}$ is the Bessel function, and $j^{-n} = \mathrm{e}^{-jn\frac{\pi}{2}}$.

Obviously, the acoustic fields of the two cylinders are different since they have different radii; we analyze the acoustic field of cylinder A at first. The acoustic field of cylinder A is composed of two parts: in the first part (denoted P_A^K), the incident wave projects onto cylinder A and then scatters back and forth between A and B, and in the other part (denoted $P_A^{K'}$), the incident wave projects onto cylinder B and then scatters back and forth between B and A.

1. The first-order acoustic field of cylinder A

Primarily, the first-order scattering field of cylinder A will be analyzed in detail in order to obtain the undetermined coefficient. In the first part, the scattered acoustic field of cylinder A in the coordinate system of A can be given as[10–13]

$$P_A^1 = \sum_{n=-\infty}^{+\infty} j^{-n}a_n\mathrm{H}_n^{(2)}(k\rho)\mathrm{e}^{jn(\varphi-\varphi')}, \quad (2)$$

where $a_n = -\mathrm{J}_n(ka)/\mathrm{H}_n^{(2)}(ka)$ for the ideally soft cylinders, $a_n = -\mathrm{J}_n'(ka)/\mathrm{H}_n'^{(2)}(ka)$ for rigid cylinders, and $\mathrm{H_n^{(2)}}(k\rho)$ is the Hankel function of the second kind.

It can be seen that there are two coordinate systems in this model, but the calculations of the total acoustic field and the boundary conditions should be carried out only under the same coordinate system. Here, we use the Graf addition theorem to express the outgoing waves from one cylinder in the coordinate system of the other.[13–15]

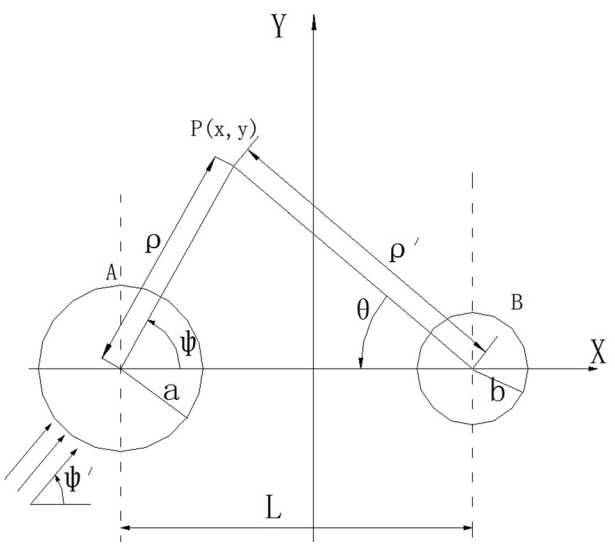

FIG. 1. Two-cylinder coordinate systems.

The first-order scattered acoustic field of cylinder A can be expressed in the coordinate system B as follows:

$$P_A^1 = \sum_{n=-\infty}^{+\infty}\left[j^{-n}a_n\mathrm{e}^{-jn\varphi'}\sum_{m=-\infty}^{+\infty}\mathrm{J}_m(k\rho')\mathrm{H}_{m+n}^{(2)}(kL)\mathrm{e}^{jm\theta}\right]. \quad (3)$$

And, in this part, the first-order scattered acoustic field of cylinder B in the coordinate system B reads

$$P_B^1 = \sum_{n=-\infty}^{+\infty} j^{-n}b_nC_n^{(1)}\mathrm{H}_n^{(2)}(k\rho')\mathrm{e}^{jn\theta}\mathrm{e}^{-jn\varphi'}, \quad (4)$$

where $b_n = -\mathrm{J}_n(kb)/\mathrm{H}_n^{(2)}(kb)$ for the ideally soft cylinders, $b_n = -\mathrm{J}_n'(kb)/\mathrm{H}_n'^{(2)}(kb)$ for rigid cylinders,[10,13] and $C_n^{(1)}$ is the undetermined coefficient in this situation.

a. Ideally soft boundary conditions. The boundary condition can be defined as follows with the problem of two ideally soft cylinders:[13]

$$(P_A^1 + P_B^1)|_{\rho'=b} = -P_B^i(\rho',\theta)|_{\rho'=b}, \quad (5)$$

which means that the total acoustic field in the coordinate system B is 0.

Combining Eqs. (3)–(5) and (1b), we can get

$$\left[\sum_{m=-\infty}^{+\infty} a_n\mathrm{J}_m(kb)\mathrm{H}_{m+n}^{(2)}(kL)\mathrm{e}^{jm\theta}\right] + b_nC_n^{(1)}\mathrm{H}_n^{(2)}(kb)\mathrm{e}^{jn\theta} = -\mathrm{J}_n(kb)\mathrm{e}^{jn\theta}, \quad (6)$$

then, the undetermined coefficient $C_n^{(1)}$ can be given by

$$C_n^{(1)} = -\frac{\left[a_n\sum_{m=-\infty}^{+\infty}\mathrm{J}_m(kb)\mathrm{H}_{m+n}^{(2)}(kL)\mathrm{e}^{jm\theta}\right] + \mathrm{J}_n(kb)\mathrm{e}^{jn\theta}}{b_n\mathrm{H}_n^{(2)}(kb)\mathrm{e}^{jn\theta}}. \quad (7)$$

Multiplying with $\mathrm{e}^{jn\theta}\mathrm{e}^{-jn\theta}$ and computing the integral in the interval $[0, 2\pi]$ at the two ends of Eq. (7), respectively, Eq. (7) can be then written again as

$$\int_0^{2\pi} C_n^{(1)}\mathrm{e}^{jn\theta}\mathrm{e}^{-jn\theta}d\theta = \int_0^{2\pi} -\frac{a_n\sum_{m=-\infty}^{+\infty}\mathrm{J}_m(kb)\mathrm{H}_{m+n}^{(2)}(kL)\mathrm{e}^{jm\theta}}{b_n\mathrm{H}_n^{(2)}(kb)}\mathrm{e}^{-jn\theta}d\theta + \int_0^{2\pi} -\frac{\mathrm{J}_n(kb)}{b_n\mathrm{H}_n^{(2)}(kb)}\mathrm{e}^{jn\theta}\mathrm{e}^{-jn\theta}d\theta, \quad (8)$$

where the left side of Eq. (8) is equal to a constant $2\pi C_n^{(1)}$, and the second term on the right side is equal to 2π, since $b_n = -\mathrm{J}_n(kb)/\mathrm{H}_n^{(2)}(kb)$. For the first term on the right side, considering that the expression $J_m(kb)\mathrm{H}_{m+n}^{(2)}(kL)/\mathrm{H}_n^{(2)}(kb)$

has nothing to do with the integral variable θ, the remaining terms will be integrated one by one. Therefore,

$$-\frac{a_n\sum_{m=-\infty}^{+\infty}\left[\mathrm{J}_m(kb)\mathrm{H}_{m+n}^{(2)}(kL)\int_0^{2\pi}\mathrm{e}^{jm\theta}\mathrm{e}^{-jn\theta}d\theta\right]}{b_n\mathrm{H}_n^{(2)}(kb)}+2\pi=2\pi C_n^{(1)}. \tag{9}$$

According to the orthogonality of the trigonometric function,[13]

$$\int_0^{2\pi}\mathrm{e}^{jm\theta}\mathrm{e}^{-jn\theta}d\theta=0\ \ (m\neq n), \tag{10a}$$

$$\int_0^{2\pi}\mathrm{e}^{jm\theta}\mathrm{e}^{-jn\theta}d\theta=2\pi\ \ (m=n), \tag{10b}$$

we can obtain that

$$C_n^{(1)}=1-\frac{a_n\mathrm{J}_n(kb)\mathrm{H}_{2n}^{(2)}(kL)}{b_n\mathrm{H}_n^{(2)}(kb)}=1+a_n\mathrm{H}_{2n}^{(2)}(kL). \tag{11}$$

Thus, the undetermined coefficient $C_n^{(1)}$ is obtained and the acoustic scattering field is determined in the case of two ideally soft cylinders.

b. Rigid boundary conditions. Compared with Eq. (5), the rigid boundary condition[13] can be changed into

$$\left.\frac{\partial(P_A^1+P_B^1)}{\partial\rho'}\right|_{\rho'=b}=\left.-\frac{\partial P^i}{\partial\rho'}(\rho',\theta)\right|_{\rho'=b}. \tag{12}$$

And, similar to the above derivation,

$$C_n^{(1)}=-\frac{\left[a_n\sum_{m=-\infty}^{+\infty}\mathrm{J}'_m(kb)\mathrm{H}_{m+n}^{(2)}(kL)\mathrm{e}^{jm\theta}\right]+\mathrm{J}'_n(kb)\mathrm{e}^{jn\theta}}{b_n\mathrm{H}'^{(2)}_n(kb)\mathrm{e}^{jn\theta}}. \tag{13}$$

Finally, the undetermined coefficient $C_n^{(1)}$ in the case of two rigid cylinders can be read as

$$C_n^{(1)}=1-\frac{a_n\mathrm{J}'_n(kb)\mathrm{H}_{2n}^{(2)}(kL)}{b_n\mathrm{H}'^{(2)}_n(kb)}=1+a_n\mathrm{H}_{2n}^{(2)}(kL), \tag{14}$$

where $a_n=-\mathrm{J}'_n(ka)/\mathrm{H}'^{(2)}_n(ka)$ and $b_n=-\mathrm{J}'_n(kb)/\mathrm{H}'^{(2)}_n(kb)$.

Especially, we can notice that when the radii of the two cylinders are the same, $C_n^{(1)}=1-\frac{a_n\mathrm{J}_n(ka)\mathrm{H}_{2n}^{(2)}(kL)}{a_n\mathrm{H}_n^{(2)}(ka)}=1+a_n\mathrm{H}_{2n}^{(2)}(kL)$, that is, the coefficient $C_n^{(1)}$ is applicable to any two infinite, parallel cylinder systems in the situation that the incident wave projects onto cylinder A and then scatters back and forth between A and B.

In the other part of the acoustic field of cylinder A (the incident wave projects onto cylinder B and then projects onto A), the undetermined coefficient $C_n^{(2)}$ can be obtained in the same way.

In this part, the scattered acoustic field of cylinder B in the coordinate system of B can be given by[10–13]

$$P_B^{1'}=\sum_{n=-\infty}^{+\infty}j^{-n}b_n\mathrm{H}_n^{(2)}(k\rho')\mathrm{e}^{jn(\theta-\varphi')}, \tag{15}$$

and the Graf addition theorem[13–15] can also be used to express it in the coordinate system A

$$P_B^{1'}=\sum_{n=-\infty}^{+\infty}\left[j^{-n}b_n\mathrm{e}^{-jn\varphi'}\sum_{m=-\infty}^{+\infty}\mathrm{J}_m(k\rho)\mathrm{H}_{m+n}^{(2)}(kL)\mathrm{e}^{jm\varphi}\right]. \tag{16}$$

The first-order scattered acoustic field of cylinder A in the coordinate system A reads

$$P_A^{1'}=\sum_{n=-\infty}^{+\infty}j^{-n}a_nC_n^{(2)}\mathrm{H}_n^{(2)}(k\rho)\mathrm{e}^{jn\varphi}\mathrm{e}^{-jn\varphi'}. \tag{17}$$

And, the boundary conditions[13] changed into

$$(P_A^{1'}+P_B^{1'})|_{\rho=a}=-P_A^i(\rho,\varphi)|_{\rho=a}\quad\text{(ideally soft)}, \tag{18a}$$

$$\left.\frac{\partial(P_A^{1'}+P_B^{1'})}{\partial\rho}\right|_{\rho=a}=\left.-\frac{\partial P_A^i}{\partial\rho}(\rho,\varphi)\right|_{\rho=a}\quad\text{(rigid)}. \tag{18b}$$

Combining Eqs. (16)–(18) and (1), we can obtain the undetermined coefficient $C_n^{(2)}$

$$C_n^{(2)}=1+b_n\mathrm{H}_{2n}^{(2)}(kL), \tag{19}$$

where $b_n=-\mathrm{J}_n(kb)/\mathrm{H}_n^{(2)}(kb)$ for the ideally soft boundary condition and for the rigid boundary condition, $b_n=-\mathrm{J}'_n(kb)/\mathrm{H}'^{(2)}_n(kb)$.[10,13]

Equations (11), (14), and (19) have a clear physical meaning. Different from the acoustic scattering field of a single cylinder, the coefficient C_n contains the interaction between two cylinders, and it can be used to reflect the multiple-scattering of each cylinder. The factor $\mathrm{H}_{2n}^{(2)}(kL)$ relates to the distance between the two cylinders: $\mathrm{H}_{2n}^{(2)}(kL)$ decreases with the increase of the wave number distance kL. We notice that $C_n=1$, when kL tends to infinity, namely the acoustic scattering field of double cylinders will degrade to a single scattering field, and the expression of one cylinder's acoustic scattering field is consistent with our previous research result.[8] In addition, Eqs. (11), (14), and (19) also contain the factors a_n and b_n, which decide the acoustic scattering coefficients of rigid or ideally soft cylinders.

2. The total scattering field of cylinder A

According to the previous derivation process and the coefficients already known, the two parts of cylinder A's acoustic scattering field can be obtained separately as,

$$P_A^K=\sum_{n=-\infty}^{+\infty}j^{-n}a_n(C_n^{(1)})^{2(K-1)}\mathrm{H}_n^{(2)}(k\rho)\mathrm{e}^{jn(\varphi-\varphi')}, \tag{20a}$$

$$P_A^{K'}=\sum_{n=-\infty}^{+\infty}j^{-n}a_n(C_n^{(2)})^{2K-1}\mathrm{H}_n^{(2)}(k\rho)\mathrm{e}^{jn[\varphi-(\varphi'-\pi)]}, \tag{20b}$$

then, the total scattering field of A can be read as $P_A=\sum_{K=1}^{+\infty}P_A^K+P_A^{K'}$, which contains the series on K.

3. The scattering field of cylinder B

The solution of cylinder B's acoustic scattering field is very similar to that of cylinder A, so we can come to the conclusion directly that

$$P_B^K = \sum_{n=-\infty}^{+\infty} j^{-n} b_n (C_n^{(1)})^{2K-1} \mathrm{H}_n^{(2)}(k\rho') \mathrm{e}^{jn\left[\theta-(\varphi'-\pi)\right]}, \quad (21a)$$

$$P_B^{K'} = \sum_{n=-\infty}^{+\infty} j^{-n} b_n (C_n^{(2)})^{2(K-1)} \mathrm{H}_n^{(2)}(k\rho') \mathrm{e}^{jn(\theta-\varphi')}, \quad (21b)$$

and the total scattering field of B can be read as $P_B = \sum_{K=1}^{+\infty} P_B^K + P_B^{K'}$. It is noticed that this result is consistent with the expression of the first-order scattering field of cylinder B, as we have calculated before.

B. Coupling characteristics of the two-cylinder system

It is already known that only more than second-order scattering fields of the two-cylinder system can be coupled.[16,17] As the higher-order acoustic scattering fields have already been obtained, we will derive the coupling coefficients with an interpretation of their physical meaning through the singularity expansion method in this section. Based on the previous results in Sec. II A,

$$P_A = \sum_{K=1}^{+\infty} P_A^K + P_A^{K'} = \sum_{n=-\infty}^{+\infty} j^{-n} a_n \mathrm{H}_n^{(2)}(k\rho) \mathrm{e}^{jn\varphi} \sum_{K=1}^{+\infty} \times \left[\mathrm{e}^{-jn\varphi'} (C_n^{(1)})^{2(K-1)} + \mathrm{e}^{-jn(\pi-\varphi')} (C_n^{(2)})^{2K-1} \right], \quad (22)$$

where

$$\sum_{K=1}^{+\infty} \left[\mathrm{e}^{-jn\varphi'} (C_n^{(1)})^{2(K-1)} + \mathrm{e}^{-jn(\pi-\varphi')} (C_n^{(2)})^{2K-1} \right] = \frac{\mathrm{e}^{-jn\varphi'}}{1-\left(C_n^{(1)}\right)^2} + \frac{\mathrm{e}^{-jn(\pi-\varphi')} C_n^{(2)}}{1-\left(C_n^{(2)}\right)^2}. \quad (23)$$

Combining Eqs. (22) and (23), the acoustic scattering field of cylinder A can be expressed as

$$P_A = \sum_{n=-\infty}^{+\infty} j^{-n} a_n M_n^A \mathrm{H}_n^{(2)}(k\rho) \mathrm{e}^{jn\varphi}, \quad (24a)$$

$$M_n^A = \frac{\mathrm{e}^{-jn\varphi'}}{1-\left(C_n^{(1)}\right)^2} + \frac{\mathrm{e}^{-jn(\pi-\varphi')} C_n^{(2)}}{1-\left(C_n^{(2)}\right)^2}, \quad (24b)$$

where M_n denotes the coupling factor of the two-cylinder system.

In the same way, the coupling factor of cylinder B can be written as

$$P_B = \sum_{n=-\infty}^{+\infty} j^{-n} b_n M_n^B \mathrm{H}_n^{(2)}(k\rho') \mathrm{e}^{jn\theta}, \quad (25a)$$

$$M_n^B = \frac{\mathrm{e}^{-jn\varphi'}}{1-\left(C_n^{(2)}\right)^2} + \frac{\mathrm{e}^{-jn(\pi-\varphi')} C_n^{(1)}}{1-\left(C_n^{(1)}\right)^2}. \quad (25b)$$

Especially, we notice that when the radii of the two cylinders are equal, $C_n^{(1)} = C_n^{(2)}$ and $M_n^A = M_n^B$. More importantly, the radii of the two cylinders affect the scattering field and the coupling coefficients of the two-cylinder system; however, they have little effect on the overall coupling characteristics. The approach we mentioned here is generally applicable to two-cylinder systems, no matter whether the radii are equal or not.

In our previous study, we have already known about the acoustic scattering field of a single cylinder[10]

$$P_z^s = \sum_{n=-\infty}^{+\infty} a_n \mathrm{H}^{(2)}{}_n(k\rho) \mathrm{e}^{jn(\varphi-\frac{\pi}{2})}. \quad (26)$$

Comparing Eqs. (24) and (26), we get

$$P^s_{\text{single}} = \sum_n P_n^s, \quad (27a)$$

$$P^s_{\text{Double}} = \sum_n P_{Dn}^s = \sum_n M_n P_n^s. \quad (27b)$$

It can be seen that different from the scattering field of a single cylinder, although the acoustic scattering field considering couplings is also composed of infinite orders of oscillation modes, there is a corresponding coupling factor M_n in each oscillation mode. What is more, since different oscillation modes correspond to different oscillation frequencies, the oscillation modes are independent of each other. It means that one coupling coefficient M_n acts only on the corresponding mode and has no effect on other modes; in other words, the coupling characteristic of the scattering field is that the scattering field is coupled by the corresponding modes of oscillation.

We have already known that the parameters of the SEM poles (l, n) represent the oscillation modes and the orders of the scattering field, respectively,[10] and then according to the coupling characteristic of two cylinders and the physical meaning of the SEM-poles, the SEM-poles are coupled depending on the parameters. That is, the poles of the same parameters are coupled, while the poles with different parameters have no interaction. Here, we come to the conclusion that the coupling characteristic of the scattering fields is the corresponding coupling between the oscillation modes of the same order, as well as the SEM poles.

The coupling characteristics of the external oscillations greatly simplify the analysis of the coupling problems and also make it possible to apply the singularity expansion method to the recognition of multiple scatterers.

III. SECOND STEP: SOLVING THE SEM POLES

We have already known that the positions of the SEM poles in the complex frequency plane are only determined by the shape and the flexible characteristics of the target,[10] and this is also applicable to the two-cylinder system. This means that the SEM poles can be used as the characteristic parameters for multiple target recognition. Therefore, it is necessary to study the pole distributions of the two-cylinder system. In this section, firstly, we will provide a physical interpretation of the SEM poles of the first and second order scattering of the

two-cylinder system. Secondly, we will obtain the approximate solution of the SEM poles by predicting the external oscillation periodic paths. Finally, the relationship between the distributions of the SEM poles and the center-to-center distance between the two cylinders will be analyzed.

A. Extraction and physical interpretation of the SEM poles

The total acoustic fields of cylinders A and B can be expressed as[18,19]

$$P_{\mathrm{A}}^{\mathrm{t}} = P_{\mathrm{A}}^{i} + P_{\mathrm{A}}^{s} = \sum_{n=-\infty}^{+\infty} j^{-n}\left[a_n M_n^A \mathrm{H}_n^{(2)}(k\rho)\mathrm{e}^{jn\varphi} + \mathrm{J}_n(k\rho)\mathrm{e}^{jn(\varphi-\varphi')}\right], \tag{28a}$$

$$P_{\mathrm{B}}^{\mathrm{t}} = P_{\mathrm{A}}^{i} + P_{\mathrm{B}}^{s} = \sum_{n=-\infty}^{+\infty} j^{-n}\left[b_n M_n^B \mathrm{H}_n^{(2)}(k\rho')\mathrm{e}^{jn\theta} + \mathrm{J}_n(k\rho')\mathrm{e}^{jn(\theta-\varphi')}\right]. \tag{28b}$$

Here, we use Watson transformation[20] to accelerate the convergence speed of the infinite series in Eq. (28). The basic idea of this approach is converting the slowly converging "canonical series" into a rapidly converging "Watson series," which is defined as a sum of residues corresponding to the complex poles of the Watson integrand.[10,21] Since we had introduced the application of Watson transformation clearly in our previous studies,[10] it will not be detailed here.

The SEM-poles of cylinder A can be determined by the denominator of $a_n M_n^A$; meanwhile, the SEM-poles of cylinder B is determined by the denominator of $b_n M_n^B$. Obviously, the solutions of the SEM-poles are completely consistent. In order to simplify the calculation, two cylinders with equal radii will be taken as an example, where $a_n = b_n$ and $M_n^A = M_n^B = \frac{\mathrm{e}^{-jn\varphi'} + (-1)^n C_n \mathrm{e}^{jn\varphi'}}{1 - C_n^2}$.

In other words, the expression of the poles is (for the ideally soft boundary condition)

$$\mathrm{J}_n(ka)\mathrm{H}_{2n}^{(2)}(kL) - 2\mathrm{H}_n^{(2)}(ka) = 0, \tag{29a}$$

and for the rigid boundary condition, Eq. (29a) changed into

$$\mathrm{J}'_n(ka)\mathrm{H}_{2n}^{(2)}(kL) - 2\mathrm{H}'^{(2)}_n(ka) = 0. \tag{29b}$$

The scattering fields obtained by Eq. (29) are the exact analytical solutions of the two-cylinder system. Compared with the scattering field expression of a single cylinder, Eq. (29) has an extra term $J_n(ka)\mathrm{H}_{2n}^{(2)}(kL)$, which will increase the orders of the equation as well as the number of SEM poles.

The exact solution of Eq. (29) is difficult in order to obtain the numerical results and the physical interpretation of the SEM poles; we obtain the approximate solutions of the SEM poles through the prediction of the external oscillation periodic paths and the application of geometrical theory of diffraction (GTD).[1,7,8]

According to the GTD, the acoustic scattering field can be separated into geometric reflected waves and diffraction waves that circumnavigated the scatterers,[8,10] so the external oscillation periodic paths can be predicted. For the two-cylinder system, the external oscillation paths will be formed as long as the external oscillation waves pass through the scattering centers of the two scatterers and constitute loops.

Only considering the first and second order scatterings, the external oscillation periodic paths can be divided into four categories, as shown in Fig. 2.

1. Total reflection between cylinders A and B

The case described in Fig. 2(a) shows the contributions associated with the closed geometrical reflection path. Since the surface reflections by the two cylinders form the external oscillation path, the SEM poles can be calculated using the following equation according to the GTD.[13]

$$\left[A(s_1)R_1\mathrm{e}^{-jks_1}\right] \times \left[A(s_2)R_2\mathrm{e}^{-jks_2}\right] = \mathrm{e}^{\pm j2n\pi}, \tag{30}$$

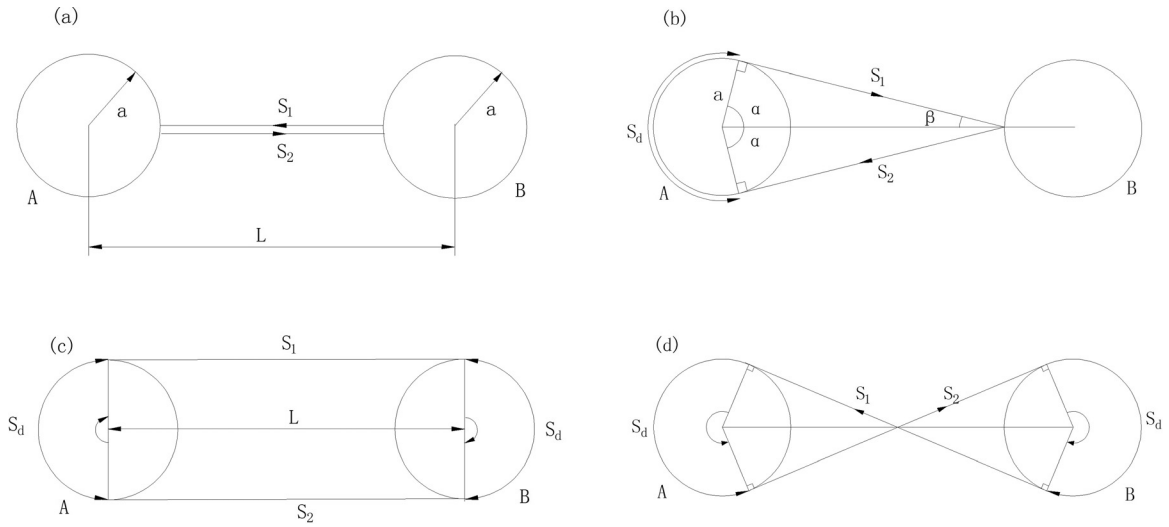

FIG. 2. External oscillation periodic paths of the first and second order scatterings of the two-cylinder system (radii a = b). (a) Geometric reflected waves, the total reflection between cylinders A and B; (b) diffraction by A and reflection by B; (c) diffraction by A and B; and (d) cross diffraction by A and B.

where $A(s)$ denotes the diffusion factor and R is the reflection coefficient. In the case of Fig. 2(a), $s_1 = s_2 = s = L - 2a$; $\rho_r = \frac{as}{2s+a}$; $A(s_1) = A(s_2) = \sqrt{\frac{s}{\rho_r+s}}$; and for the ideally soft boundary condition, $R_1 = R_2 = 1$; for the rigid boundary condition, $R_1 = R_2 = -1$.

Figure 3 displays the comparison between the exact and approximate results of SEM pole distributions. It is associated with the first order geometrical reflection presented in Fig. 2(a). The analytical solutions are derived from Eq. (29) and the approximate solutions are derived from Eq. (30). We observe good agreement between the SEM poles computed by the two different methods.

2. Diffraction by A and reflection by B

Figure 2(b) displays the external oscillation orbits made up of a geometric field and a diffraction field. According to the GTD,[13] the distributions of the SEM poles in this case can be expressed as

$$E^d(s_d)A(s_1)R \times A(s_2)\mathrm{e}^{-jk(s_2+s_2)} = \mathrm{e}^{\pm j2n\pi}, \tag{31a}$$

where $E^d(s_d)$ denotes the first-order creeping waves surrounding the surface of cylinder A, and

$$E^d(s_d) = 4.07\left(\frac{ka}{2}\right)^{\frac{1}{3}}\mathrm{e}^{\frac{j\pi}{6}}\mathrm{e}^{-j\vartheta_1(ka)\frac{s_d}{a}}, \tag{31b}$$

$$A(s_1) = (8j\pi k \times s_1)^{-\frac{1}{2}}, \tag{31c}$$

$$A(s_2) = \left(\frac{s_2}{\rho_r + s_2}\right)^{\frac{1}{2}}, \tag{31d}$$

where $\vartheta_1(ka)$ are the zeros of Hankel functions of the second kind on the complex k plane for the ideally soft boundary condition, and for the rigid boundary condition, $\vartheta_1(ka)$ changed into the zeros of the derivative of the Hankel function of the second kind.[1,7,8,13]

In the case shown in Fig. 2(b), $s_1 = s_2 = a\tan\alpha$; $\rho_r = \frac{as_1}{2s_1\cos\beta+a}$; $\alpha = \arccos\frac{a}{L-a}$; $\beta = \frac{\pi}{2} - \alpha$; and $s_d = a \times 2(\pi - \alpha)$.

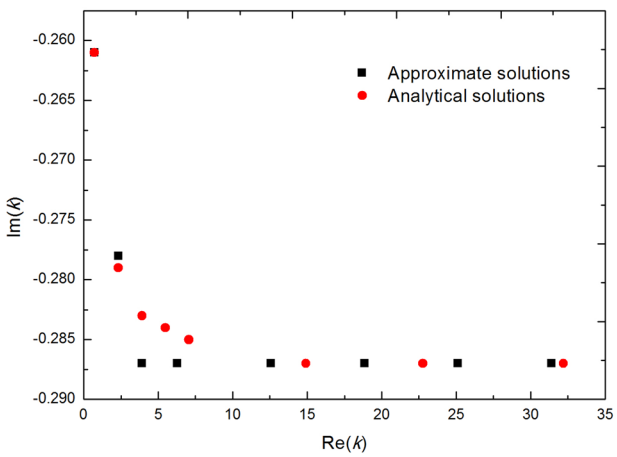

FIG. 3. Exact solutions and approximate solutions in the complex k plane associated with the first order geometrical reflection. (Ideally soft boundary condition, separation distance $L = 6a$.)

3. Diffraction by A and B

Figure 2(c) displays the external oscillation orbits made up of two diffraction fields. According to the GTD, the distributions of the SEM poles in this case can be expressed as[13]

$$\left[M^d(s_d)A(s)R \times \mathrm{e}^{-j\vartheta_1(ka)\frac{s_d}{a}}\mathrm{e}^{-jks}\right]^2 = \mathrm{e}^{\pm j2n\pi}, \tag{32a}$$

$$M^d(s_d) = 4.07\left(\frac{ka}{2}\right)^{\frac{1}{3}}\mathrm{e}^{\frac{j\pi}{6}}, \tag{32b}$$

$$A(s) = (8j\pi k \times s)^{-\frac{1}{2}}. \tag{32c}$$

In the case shown in Fig. 2(b), $s = L$ and $s_d = a\pi$.

4. Cross diffraction by A and B

Figure 2(d) displays that the external oscillation orbits are also made up of two diffraction fields, but these two diffraction fields are crossed. According to the GTD,[13] the formula for calculating the distributions of the SEM poles is the same as Eq. (32), but the geometric parameters have changed into $s_d = a \times \left(2\pi - 2\arccos\frac{2a}{L}\right)$ and $s = 2[(\frac{L}{2})^2 - a^2]^{\frac{1}{2}}$.

Figure 4 displays the distributions of the SEM poles calculated by Eqs. (31) and (32). It is associated with other three external oscillation orbits presented in Figs. 2(b)–2(d). Comparing Figs. 3 and 4, it can be seen that the poles associated with the geometrical reflection path are the closest to the real axis. This is because the wave attenuation of this path is the smallest. Meanwhile, the diffraction distance of the other three external oscillation orbits increases gradually, and this leads to the gradual increase of the wave attenuation in the three orbits. Therefore, the SEM poles corresponding to these three orbits are farther and farther away from the real axis. These conclusions are consistent with the results of our previous studies on the distribution characteristics of the SEM-poles.[10]

5. The distributions of SEM-poles with different radii

Figure 5 displays the external oscillation periodic paths of the two-cylinder system with different radii. Comparing

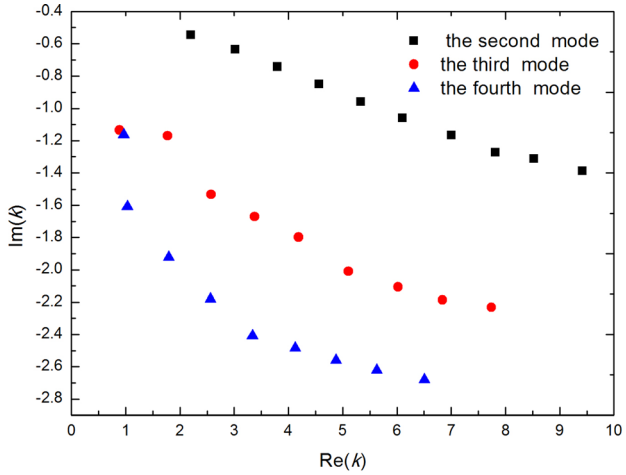

FIG. 4. The distributions of the SEM poles in the complex k plane corresponding to the other three external oscillation periodic paths. (Ideally soft boundary condition, separation distance $L = 6a$.)

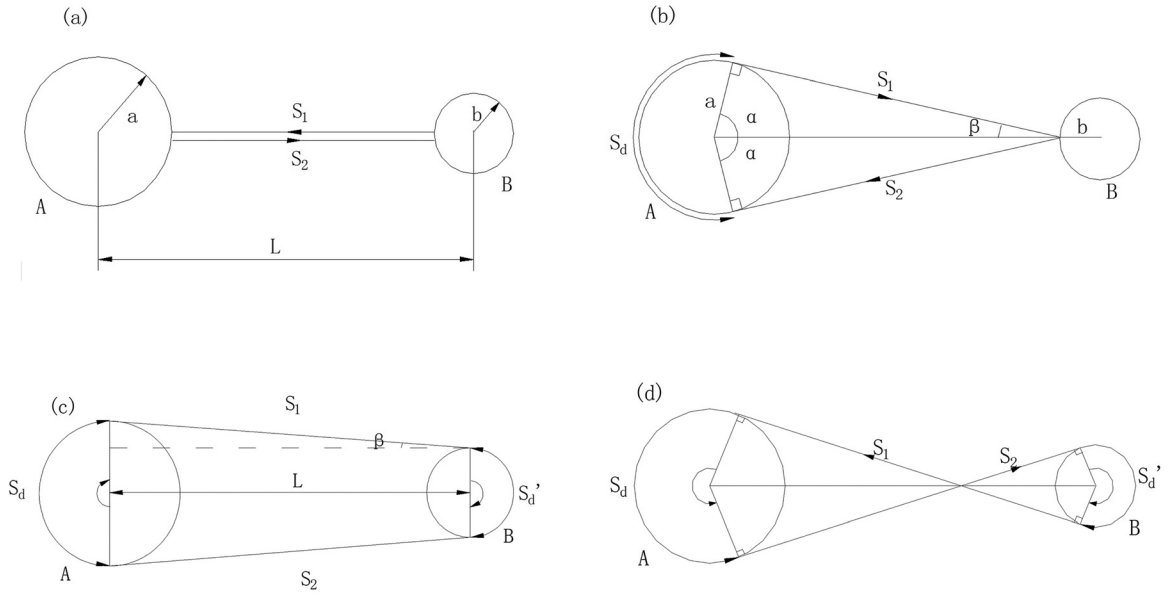

FIG. 5. External oscillation periodic paths of the first and second order scatterings of the two-cylinder system (radii a ≠ b). (a) Geometric reflected waves, total reflection between cylinders A and B; (b) diffraction by A and reflection by B; (c) diffraction by A and B; and (d) cross diffraction by A and B.

Figs. 2 and 5, it can be seen that when radii a ≠ b, the calculation methods of the SEM-poles are the same, but the geometric parameters are significantly different. This not only leads to the difference in the SEM-pole distributions between single and double cylinder systems, but also leads to the difference in the pole distributions between cylinders A and B.

Take Fig. 5(a) as an example, the SEM poles can also be calculated using Eq. (30), but the geometric parameters changed into: $s_1 = s_2 = s = L - a - b$; $\rho_r^A = \frac{as}{2s+a}$; $\rho_r^B = \frac{bs}{2s+b}$; $A(s_1) = \sqrt{\frac{s}{\rho_r^A + s}}$; $A(s_1) = \sqrt{\frac{s}{\rho_r^B + s}}$. It should be noted that the pole distributions of cylinders A and B calculated by the external oscillation paths shown in Fig. 5(a) are the same; however, they are quite different in the other three cases.

The distributions of the SEM poles corresponding to the second external oscillation paths [shown in Fig. 5(b)] can be calculated using Eq. (31), and the geometric parameters of cylinder A do not change. While the geometric parameters of cylinder B change to $s_1' = s_2' = b \tan \alpha'$; $\rho'_r = \frac{bs'_1}{2s'_1 \cos \beta' + b}$; $\alpha' = \arccos \frac{b}{L-b}$; $\beta' = \frac{\pi}{2} - \alpha'$; and $s'_d = b \times 2(\pi - \alpha')$.

Figure 6(a) displays the pole distributions of the two cylinders when the radii a = b and a = 4b, respectively (corresponding to the first external oscillation periodic path), and Fig. 6(b) displays the pole distributions of cylinders A and B, respectively, when the radii a = 4b (corresponding to the second external oscillation periodic path). From Fig. 6, we can see that the trends of the curves are consistent, but the imaginary parts of the poles are reduced. The other two modes of the external oscillations have similar calculation methods for the pole distributions, which will not be described in detail herein.

B. The relationship between the separation distance and the SEM poles

The poles closest to the real axis correspond to the first order geometrical reflections, and they are the easiest to be

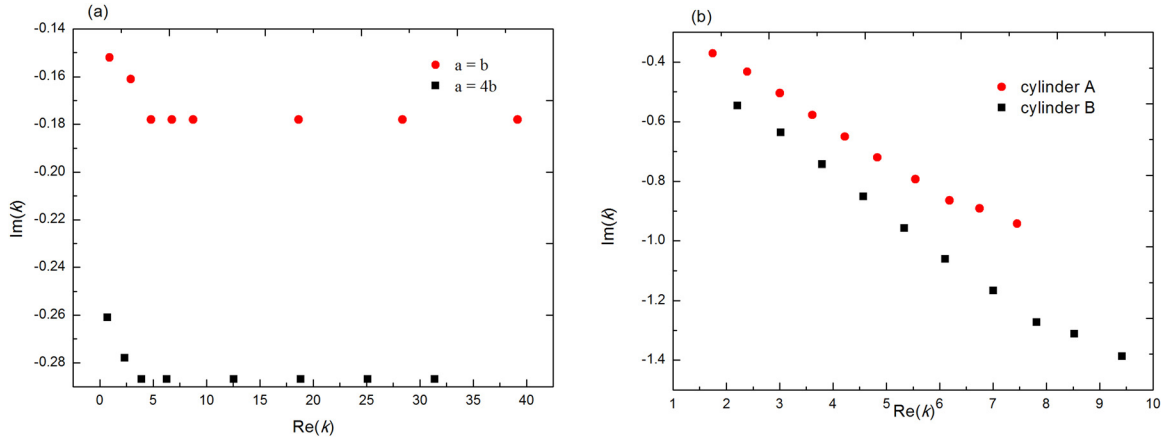

FIG. 6. (a) Influence of the radii on the distributions of the SEM poles corresponding to the first external oscillation periodic path. (b) The SEM-pole distributions of cylinders A and B when radii a = 4b, corresponding to the second external oscillation periodic path. (Ideally soft boundary condition, separation distance $L = 6a$.)

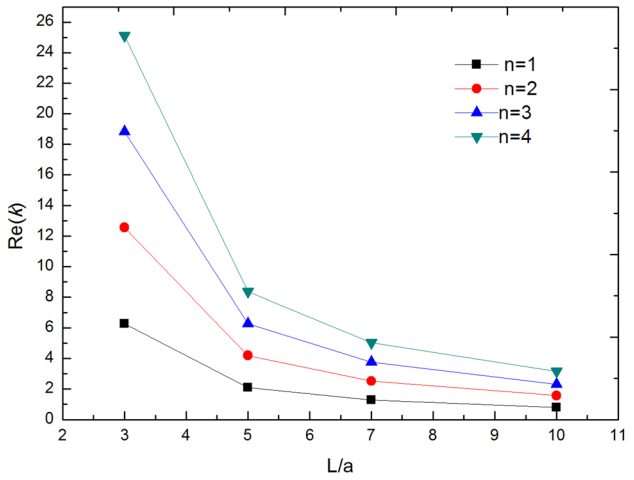

FIG. 7. The relationship between the separated distance and the real parts of the SEM poles.

extracted in numerical calculations and experiments. The distributions of the poles directly reflect the distance between the scatterers. So, the distance between the two cylinders can be recognized by the distribution characteristics of the poles. Figure 7 shows the change in the real parts of the poles accompanied by the change in the distance between the two cylinders. Obviously, when the separation distance L increases, the real parts of the poles have a significant decrease. This arises because the wavelength of every standing wave formed by the external oscillations is directly proportional to the diffraction distance, but is inversely proportional to the oscillation frequency. Hence, an increase in the diffraction distance leads to an increase in the standing-wave wavelength and a decrease in the oscillation frequency represented as the real parts of the poles.[8]

This relationship can be used to recognize the location information of the two scatterers.

IV. CONCLUSIONS

With a general two-cylinder system as an example, we have proposed an approach to perform the multiple-scattering calculations of the two-cylinder acoustic scattering problem and extracted the coupling factors and analytical solutions of the SEM poles by using the singularity expansion method. We have also obtained the poles through interpreting the coupling characteristics of the external oscillations, which are consistent with the exact results. We note that the coupling characteristic of the scattering field is the corresponding coupling between the oscillation modes of the same order, as well as the SEM poles. The coupling characteristics of the external oscillations greatly simplify the analysis of the coupling problems, and also make it possible to apply the singularity expansion method to the recognition of multiple scatterers. By interpreting the physical meaning of the coupling coefficients and explaining the influence of the coupling characteristics to the pole distributions, we come to the conclusion that this approach can be used to solve the pole distributions of multiple scatterers in acoustic scattering problems and study the characteristics of the external oscillations of multiple scatterers. In addition, we have also briefly analyzed the relationship between the real parts of the SEM poles and the separated distance.

Based on the approach presented in this paper, we will further consider the relationship between the distributions of the SEM-poles and the geometrical characteristics of multiple scatterers and use the SEM poles as the characteristic parameters for multiple target recognition. We will also focus on scatterers with complex boundary conditions and geometrical characteristics. This new method and related calculation results lay the foundation of structural design and noise analysis for multiple scatterers in engineering, may provide an effective means to recognize shapes in acoustic scattering fields, and could have potential applications in non-destructive testing and acoustic imaging.

ACKNOWLEDGMENTS

The authors would like to thank the National Natural Science Foundation of China (Grant No. 51675401) for financial support.

[1]P. Gabrielli and M. Mercier-Finidori, Phys. Rev. E **66**, 046629 (2002).
[2]V. Twersky, J. Acoust. Soc. Am. **24**, 42 (1952).
[3]E. Burke, D. Censor, and V. Twersky, J. Acoust. Soc. Am. **37**, 5 (1965).
[4]J. Young and J. Bertrand, J. Acoust. Soc. Am. **58**, 1190 (1975).
[5]J. B. Keller, J. Opt. Soc. Am. **52**, 116 (1962).
[6]G. Vattay, A. Wirzba, and P. E. Rosenqvist, Phys. Rev. Lett. **73**, 2304 (1994).
[7]A. Wirzba, Nucl. Phys. A **560**, 136 (1993).
[8]A. Wirzba, Phys. Rep. **309**, 1 (1999).
[9]A. K. Hamid, J. Electromagn. Waves Appl. **18**, 1427 (2004).
[10]P. Cao and J. H. Wu, J. Appl. Phys. **121**, 105103 (2017).
[11]E. Heyman and L. Felsen, IEEE Trans. Antennas Propag. **33**, 706 (1985).
[12]G. Gaunaurd and H. Überall, J. Acoust. Soc. Am. **78**, 234 (1985).
[13]G. R. Yang, *Advanced Electromagnetic Theory* (Higher Education Press, Beijing, China, 2008).
[14]Y. A. Ivanov, *Diffraction of Electromagnetic Waves on Two Bodies* (National Aeronautics and Space Administration, Washington, DC, 1970).
[15]S. M. Hasheminejad and M. Azarpeyvand, "Acoustic radiation from a cylindrical source close to a rigid corner," Z. Angew. Math. Mech. **85**(1), 66–74 (2005).
[16]G. Kapodistrias and P. H. Dahl, J. Acoust. Soc. Am. **107**, 3006 (2000).
[17]A. O. Maksimov and V. I. Yusupov, Eur. J. Mech. - B/Fluids **60**, 164 (2016).
[18]H. A. Ragheb and M. Hamid, Int. J. Electron. **59**, 407 (1985).
[19]J. A. Roumeliotis and V. Douvalis, J. Electromagn. Waves Appl. **18**, 591 (2004).
[20]G. N. Watson, Proc. R. Soc. London, Ser. A **95**, 83 (1918).
[21]C. E. Baum, "On the singularity expansion method for the solution of electromagnetic interaction problems," in *Interaction Note 88* (Air Force Weapons Laboratory, 1971).